Mem. S.A.It. Vol. 00, 0
© SAIt 2008
Memorie della

arXiv:0910.4260v1 [astro-ph.HE] 22 Oct 2009

The nature of the 4th track in GX 5-1: discovery of Fe XXVI RRC in massive flares

M. J. Church[1,2], O. Dimbylow[1], C. Peach[1], and M. Balucinska-Church[1,2]

[1] School of Physics & Astronomy, University of Birmingham, Birmingham B15 2TT, UK
[2] Astronomical Observatory, Jagiellonian University, ul. Orla 171, 30-244, Cracow, Poland
e-mail: mjc@star.sr.bham.ac.uk

Abstract. We present an explanation of the 4th branch of the Z-track based on analysis of high-quality *RXTE* data on the source GX 5-1. Spectral analysis shows that the physical evolution on the 4th track is a continuation of the flaring branch which we previously proposed consists of unstable nuclear burning of the accretion flow on the neutron star. In flaring there is a huge increase of the neutron star emission from a volume that increases to a radius of 21 km. The 4th branch is shown to consist of flaring under conditions that the mass accretion rate and thus the total source luminosity is falling. We detect strong emission on the flaring and 4th branches at energies between 7.8 - ~9.4 keV inconsistent with origin as Fe K emission, which we suggest is the radiative recombination continua (RRC) of iron Fe XXVI at 9.28 keV and of lower states. Evolution of the emission takes place, the energy falling but the flux increasing strongly, consistent with production in the large volume of unstable nuclear burning around the neutron star which eventually cools.

Key words. Physical data and processes: accretion: accretion disks — stars: neutron — stars: individual: GX 5-1 — X-rays: binaries

1. Introduction

The Z-track sources form the brightest group of Low Mass X-ray Binary (LMXB) sources containing a neutron star, including: GX 340+0, GX 5-1, Cyg X-2, Sco X-1, GX 17+2 and GX 349+2 (Hasinger & van der Klis 1989). All of these persistently radiate at or above the Eddington limit for a neutron star. The sources trace a Z-shaped pattern in X-ray hardness versus intensity consisting of the horizontal branch (HB), the normal branch (NB) and the flaring branch (FB). The sources are divided into the Cyg-like sources: GX 340+0, GX 5-1 and Cyg X-2 with long horizontal branches and the Sco-like sources: Sco X-1, GX 17+2 and GX 349+2 with short horizontal branches but stronger flaring branches. This strong hardness evolution along the Z-track is clearly due to major physical changes taking place within the sources, the nature of which has not been understood. However, based on analysis of *Rossi-XTE* data on the sources GX 340+0, GX 5-1 and Cygnus X-2, we have proposed a model of the Cyg-like sources (Church et al. 2006; Jackson et al. 2008, Bałucińska-Church et al. 2009). In this model, the increase in X-ray intensity moving on the NB from the soft apex to the hard apex is due to an increase of mass accretion rate. There is a resultant heating of the

Send offprint requests to: M. J. Church

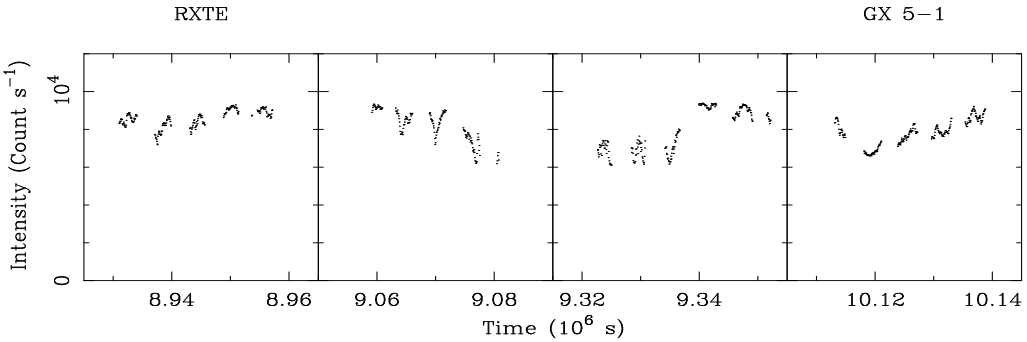

Fig. 1. Lightcurve of the observation in the energy band 1.9 - 18.5 keV. The data consist of 4 sub-observations so that, to improve clarity, the gaps between the sub-observations have been compressed.

neutron star and a contraction in the emitting area so that the flux emitted per unit area of the neutron star surface becomes super-Eddington leading to disruption of the inner disk and the launching of jets detected as radio emission on this part of the Z-track. On the FB, spectral fitting showed little change of $\dot{M}$ but the large increase in the luminosity of the neutron star indicated unstable nuclear burning on the neutron star. Moreover there was good agreement at the onset of flaring (the soft apex) between the mass accretion rate per unit area of the neutron star $\dot{m}$ and the theoretical value below which burning of the accretion flow on the neutron star becomes unstable.

In addition, the Cyg-like sources sometimes display extra unusual tracks which similarly have not been understood. In Fig. 2 we show the additional 4th branch in GX 5-1 in the observation analysed in the present work. It can be seen that this begins at the end of the FB and moves in the direction of decreasing hardness and decreasing intensity. It has been referred to as the "dipping track" because of the decreasing intensity (e.g. Kuulkers & van der Klis 1996) by analogy with the dipping class of LMXB in which absorption in the bulge in the outer disk causes orbital-related decreases of intensity. This absorption may cause a hardening of the spectrum, but energy-independent dipping (Church & Bałucińska-Church 1993) and also softening (Church & Bałucińska-Church 1995) in dips is also observed. This range of behaviour may be explained in terms of two continuum emission components within the sources (Church & Bałucińska-Church 1995). The apparent dipping in a Z-track source led to the suggestion that the Cyg-like sources have high inclination and that this explains the difference between the Cyg-like and Sco-like sub-groups. It should be noted, however, that we would not expect the 4th track to be associated with flaring but to take place on any part of the Z-track.

In the present work, we carry out an investigation of the 4th track in GX 5-1.

2. Observations and analysis

The observations analysed were made using *RXTE* in October and November 1996. The lightcurve of these observations is shown in Fig. 1 and the corresponding Z-track is shown in Fig. 2 in which the hardness ratio is obtained by the division of light curves in the bands 10.2 - 17.5 and 6.5 - 10.2 keV. Spectra were accumulated as a function of position along the Z-track by defining boxes in hardness-intensity typically 0.005 wide in hardness and 100 count s^{-1} wide in intensity. Two spectra were chosen on the HB, one at the hard apex, two on the NB, one at the soft apex, two on the FB, one at the 3rd apex and three others on the 4th track.

In our previous work on the three Cygnus X-2 like sources (Church et al. (2006); Jackson et al. (2008); Bałucińska-Church et al. 2009) we showed that spectral evolution along

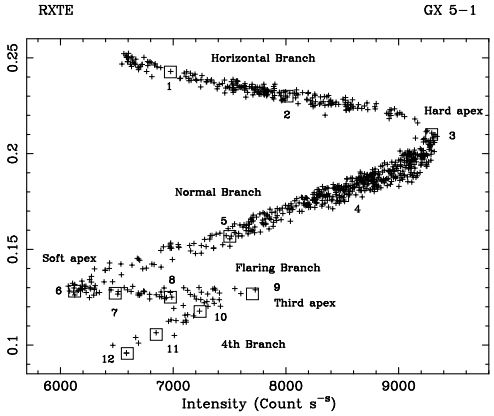

Fig. 2. Z-track of the observations analysed showing the fourth track in GX 5-1.

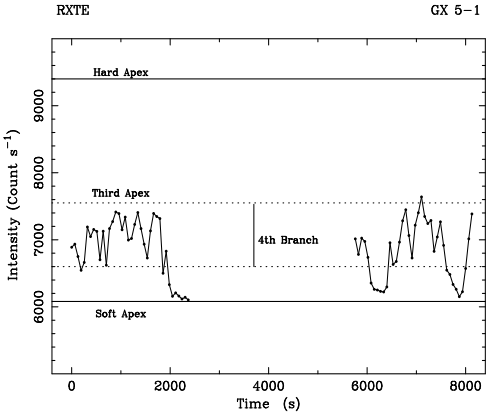

Fig. 3. The part of the lightcurve during which the source moves on the 4th branch.

the Z-track was well-described by application of the Extended ADC emission model for low mass X-ray binaries (Church & Bałucińska-Church 2004) in which the continuum emission comprises the blackbody emission of the neutron star and the dominant Comptonized emission of the extended accretion disk corona (ADC). Application of this model suggested a clear physical explanation of the Z-track as summarised in Sect. 1. Thus this model was applied in the present work in the form AB∗ (BB + CUT) where BB is the blackbody emission of the neutron star, CUT is a cut-off power law description of Comptonization is an extended accretion disk corona (Church & Bałucińska-Church 2004) and AB is absorption. This model provided good fits on the HB and NB, however, on the flaring branch and in particular on the 4th branch, strong, broad line emission became apparent at energies above 9 keV. This was modelled using the REDGE model in *Xspec* for the recombination radiation continuum (RRC) emitted following recombination of highly ionized states of ions, particularly of iron, since such transitions from the continuum to the ground state have energies above 9 keV.

3. Results

In Fig. 3 we show that part of the lightcurve of the source during which the source moves on the 4th branch. Horizontal lines are drawn at

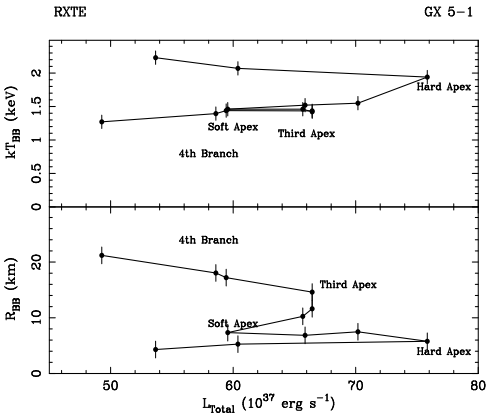

Fig. 4. Evolution of neutron star blackbody temperature (upper panel) and blackbody radius (lower panel) along the Z-track.

the intensities of the soft apex, the third apex and the end of the 4th branch. In the second block of data it can be seen that the source moves from the soft apex in strong flaring up to the third apex. It then moves several times between the third apex and the end of the 4th branch eventually returning to the soft apex. We will show that although the intensity decreases from the 3rd apex to the end of the 4th branch, the neutron star luminosity in fact *increases strongly* so that the 4th branch actually consists of a continued strong increase of flare intensity, i.e. of the neutron star luminosity.

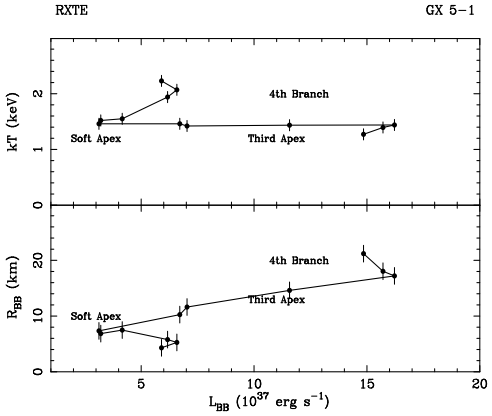

Fig. 5. The unfolded evolution of $kT_{\rm BB}$ (upper panel) and $R_{\rm BB}$ (lower panel) as a function of blackbody luminosity (see text).

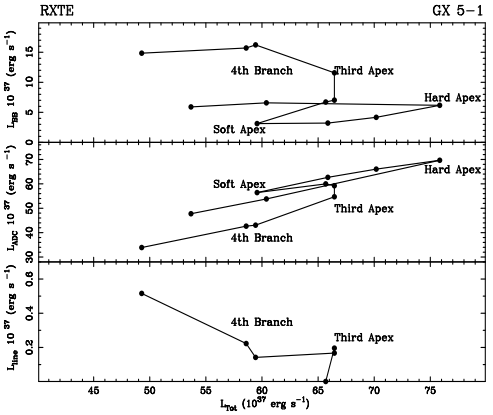

Fig. 6. Evolution of the neutron star blackbody luminosity (upper); the ADC Comptonized emission (middle) ; the emission line (lower).

Spectral fitting results are shown in Fig. 4 for the neutron star blackbody temperature $kT_{\rm BB}$ (upper panel) and blackbody radius $R_{\rm BB}$ (lower panel) as a function of the total luminosity in the band 1 - 30 keV. The behaviour on the NB and HB is the same as found by Jackson et al. (2008), i.e. on the NB, $kT_{\rm BB}$ increases from a low value at the soft apex (1.5 keV) to a high value on the HB end of the Z-track (2.2 keV). At the same time the blackbody radius $R_{\rm BB}$ decreases from a value approaching the radius of the neutron star to a much smaller value. On the FB and the 4th branch, the behaviour of both $kT_{\rm BB}$ and $R_{\rm BB}$ is monotonic, the major effect being the increase of $R_{\rm BB}$.

The difference between the FB and the 4th branch is clearly the strong decrease in total luminosity on the 4th branch. The results are more clearly seen if we show them separately from this decrease of $L_{\rm Tot}$ which is done by replotting as a function of the blackbody luminosity $L_{\rm BB}$ as shown in Fig. 5.

It can be seen in Fig. 5 that this unfolds the data and makes it clear that the behaviour on the 4th branch is a continuation of that seen on the FB, i.e. the 4th track is a continuation of flaring, which becomes very strong on the 4th track, i.e. there is a strong increase in the blackbody emission of the neutron star. The emission has increasing area, and on the 4th track $R_{\rm BB}$ becomes very much greater than the neutron star radius, rising to a maximum of 21 km.

In Fig. 6 we show the variation of the luminosity components: the neutron star blackbody luminosity $L_{\rm BB}$ (upper panel) and the luminosity of the ADC Comptonized emission $L_{\rm ADC}$ (middle panel) with $L_{\rm Tot}$. There is a strong increase of $L_{\rm BB}$ on the flaring branch which is continued on the 4th branch. However, at the third apex, $L_{\rm ADC}$ has begun to decrease and on the 4th branch decreases strongly. The lower panel shows the strong emission feature seen on the 4th branch modelled as RRC emission (below); this rose to 15% of the neutron star luminosity or 4% of the total luminosity.

The reason for the down-curving of the 4th track thus becomes clear: the overall luminosity decreases because the Comptonized ADC emission is decreasing. Because $L_{\rm ADC}$ is ~90% of the total luminosity (at the soft apex), the decrease on the 4th track is a firm indicator that the mass accretion rate $\dot{M}$ decreases. Thus the 4th track is simply the occurrence of strong flaring, i.e. unstable nuclear burning, under conditions of decreasing $\dot{M}$.

The spectra on the 4th branch clearly displayed strong broad emission which could be well-fitted by addition of a Gaussian line. In the 4 spectra spaced along the 4th track beginning at the third apex, the line energies were 9.49±0.67, 9.72±0.57, 8.80±0.25 and

7.58±0.78 keV. The equivalent width increased from 320 eV to 1480 eV along the 4th branch. However, these energies are not consistent with Fe K emission but are suggestive of Fe radiative recombination continuum (RRC) characteristic of the various edges of highly ionized Fe. Consequently, we fitted the emission using the REDGE model in *Xspec*. This model produced equally good quality fits; results are shown in Table 1 and a typical fit in Fig. 7.

Table 1. Results of fitting the REDGE model

spectrum	edge energy (keV)	kT_e (keV)
9	8.98±0.27	1.03±0.28
10	9.39±0.22	0.76±0.22
11	8.58±0.17	0.86±0.15
12	7.77±0.09	1.13±0.13

In this model the free parameters are the edge energy, the line normalization and the temperature kT_e of the recombining electrons which determines the width. The edge energies associated with recombination of highly ionized states of Fe to the next lower state are shown in Table 2 (Kallman 2003).

Table 2. Edge energies for RRC in Fe

edge energy (keV)	state	edge energy (keV)	state
9.278	Fe XXVI	8.088	Fe XIX
8.755	Fe XXV	7.989	Fe XVIII
8.621	Fe XXIV	7.891	Fe XVII
8.482	Fe XXIII	7.838	Fe XVI
8.384	Fe XXII	7.788	Fe XV
8.286	Fe XXI	7.737	Fe XIV
8.187	Fe XX	7.686	Fe XIII

The detected emission in spectrum 10 implies RRC emission of Fe XXVI recombination falling at the end of the 4th branch to Fe XI. At any stage a mixture of states will probably be present, and spectrum 12 at the flare peak was not well fitted with a single RRC, providing some evidence of this. In this case the fitting results may not give the electron temperature.

The presence of the emission only in flaring clearly shows it is associated with flaring which we have suggested is unstable nuclear burning. It becomes strong on the 4th branch where flaring is very strong. The increase in strength may well be due to the increase of blackbody radius of the neutron star emission. Thus if there is unstable nuclear burning that creates a fireball around the neutron star extending to a radius of ~21 km (Fig. 3) there will be a large volume in which the line can be generated. The decrease of edge energy towards the end of the 4th branch correlates with the fall of kT_{BB} implying an eventual cooling.

4. Discussion

Our analysis of GX 5-1 shows that the 4th branch is simply a continuation of the flaring branch in which the behaviour of the neutron star blackbody temperature kT_{BB} and radius R_{BB} continues on the 4th branch as on the flaring branch, as shown in Fig. 4. On the 4th branch, L_{ADC} decreases showing that $\dot{M}$ decreases, so that the increase of L_{BB} can only be due to nuclear burning on the surface of the neutron star. We previously showed that in the three Cygnus X-2 like sources (e.g. Church et al. 2006), at the soft apex, the value of $\dot{m}$, the mass accretion rate per unit area of the neutron star, agreed well with the critical value below which nuclear burning is unstable (e.g. Bildsten 1998). Thus as the source moves along the NB to the soft apex, unstable burning starts and the FB is formed. The presence of a 4th branch shows that $\dot{M}$ continues to fall and the 4th branch is a combination of unstable burning and this.

The observation of strong emission at energies between 7.8 and ~9.4 keV is of great interest. We suggest that this is RRC emission of ionization states Fe XXVI and lower levels. Recombination of H-like Fe to He-like Fe produces RRC at 9.28 keV consistent with the peak emission energy observed. The emission is very strong which may be due to the large volume of emitting plasma around the neutron star suggested by the large values of blackbody radius of up to 21 km. The decrease of line energy towards the end of the 4th track indicates

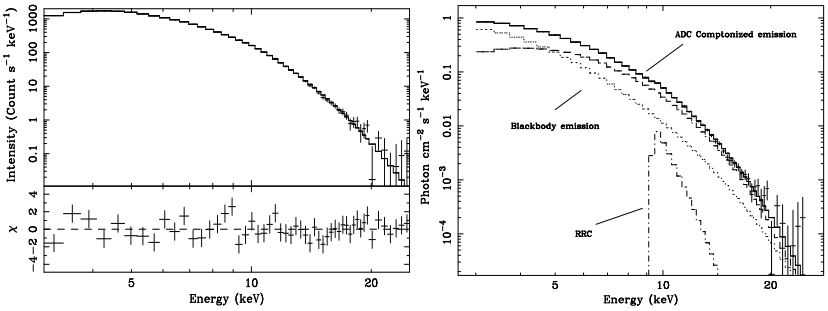

Fig. 7. Modelling of the emission feature at ~9.5 keV in spectrum 10 with RRC emission: left: folded spectrum with residuals; right: the unfolded spectrum.

cooling as does the fall of blackbody temperature at the end of the 4th track.

The detection of Fe RRC is very rare in Galactic sources. However, a broad line at ~10 keV was previously seen in GX 5-1 on the flaring and 4th branch by Asai et al. (1994), probably the same feature as we have detected. They considered possible origin of the line as Fe Kα, shifted to higher energies, either by a Doppler shift in the disk, or by Compton scattering or by blue-shifting in a jet, but none of these could provide a satisfactory explanation.

A strong, broad feature at 9.28 keV has previously been seen in gamma ray bursts. In GRB 970828, a broad emission feature at 4.8 keV corrected for the well-determined redshift of the host galaxy of z = 0.9578 corresponds closely to 9.28 keV (Yoshida et al. 2001). kT_e in this case was 0.8 keV producing a very broad feature. Weth et al. (2000) considered conditions under which the emission at 9.28 keV can be strong. In Galactic sources, narrow RRC emission of O VIII and O VII was seen in the dipping source XBT 0748-676 (Cottam et al. (2001) and in planetary nebulae (Nordon et al. 2009) in which kT_e is only a few eV.

In our case, the peak energy on the 4th branch corresponds to Fe XXVI RRC, i.e. H-like iron and it appears that this emission is associated with the fireball around the neutron star resulting from uncontrolled nuclear burning. Further detailed study is clearly required.

Acknowledgements. This work was supported in part by the Polish grant 3946/B/H03/2008/34.

References

Asai, K., Dotani, T., Mitsuda, K., Nagase, F., et al. 1994, PASJ, 46, 479
Bałucińska-Church, M., Gibiec, A., Jackson, N. K., Church, M. J. 2009, A&A, submitted
Bildsten, L., 1998, in Proc NATO ASIC 515, The Many Faces of Neutron Stars, eds. R. Buccheri, J. van Paradijs & M. A. Alpar, Dordrecht-Kluwer, 419
Church, M. J., Bałucińska-Church, M. 1993, MNRAS, 260, 59
Church, M. J., Bałucińska-Church, M. 1995, A&A, 300, 441
Church, M. J., Bałucińska-Church, M. 2004, MNRAS, 348, 955
Church, M. J., Halai, G. S., Bałucińska-Church, M. 2006, A&A, 460, 233
Cottam, J., Kahn, S. M., Brinkman, A. C., den Herder, J. W., Erd, C. 2001, A&A, 365, L277
Hasinger, G., van der Klis, M. 1989, A&A, 225, 79
Jackson, N. K., Church, M. J., Bałucińska-Church, M. 2008, A&A, 494, 1059
Kuulkers, E., van der Klis, M. 1996, 314, 567
Kallman, T. 2003, http://heasarc.gsfc.nasa.gov/W3Browse/physics-data/edgeenergy.html
Nordon, R., Behar, E., Soker, N., Kastner, J. H., Yu, Y. S. 2009, ApJ, 695, 834
Yoshida, A., Namiki, M., Murakami, T., et al. 2001, ApJ, 557, L27
Weth, C., Mészáros, P., Kallman, T., Rees, M. J. 2000, ApJ, 534, 581